Selective Doping of Photochromic Dye into Nanostructures of Diblock Copolymer Films by Vaporization in a Vacuum

Toshiko Mizokuro,*,† Hiroyuki Mochizuki,† Atsuko Kobayashi,† Shin Horiuchi,‡ Noritaka Yamamoto,† Nobutaka Tanigaki,† and Takashi Hiraga†

Photonics Research Institute, National Institute of Advanced Industrial Science and Technology (AIST), Kansai, Midorigaoka 1-8-31 Ikeda, Osaka 563-8577, Japan, and Nanotechnology Research Institute, AIST, Tokyo Waterfront, 2-41-6, Aomi, Kohtoh-ku, 135-0064 Tokyo, Japan

Received March 16, 2004. Revised Manuscript Received June 30, 2004

Poly(phenyl methacrylate) (PPhMA), poly(methyl methacrylate) (PMMA), poly(*tert*-butyl methacrylate), polystyrene (PS), poly(4-methylstyrene), poly(p-*tert*-butylstyrene), and polycarbonate (PC) were doped with the photochromic dye *cis*-1,2-dicyano-1,2-bis(2,4,5-trimethyl-3-thienyl)ethene (CMTE) using a simple vacuum process termed the "vapor transportation method." The CMTE-doped polymer molds and powder were examined by optical microscopy, SEM/energy-dispersive X-ray (EDX) elemental analysis, Fourier transform infrared absorption (FT-IR), and transmission electron microscopy (TEM). CMTE-doped PS, PC, and PMMA molds showed photochromism. Optical microscopy and sulfur (S) elemental analysis confirmed formation of CMTE-doped regions, with rapid CMTE concentration decreases at the CMTE-doped region/polymer substrate interface. CMTE doping rates into PS, PC, and PMMA were estimated by measuring the depths of the doped regions. CMTE showed more efficient penetration into PS than into PC or PMMA. FT-IR measurements showed saturated concentrations of CMTE in the CMTE-doped polymer powder. PS and PPhMA, with phenyl groups in their side chains, showed the highest concentrations of CMTE among PS derivatives and PMMA derivatives, respectively. Our results indicated that the affinity between CMTE and aromatic groups in these polymers, based on "$\pi-\pi$ interactions," enhances CMTE doping. Ultrathin sectioned TEM images of CMTE-doped diblock copolymers, "PS-rich PS-*block*-PMMA (PS-*b*-PMMA)," and CMTE-doped "PMMA-rich PS-*b*-PMMA" films confirmed that CMTE was dispersed selectively into PS nanodomains in "PMMA-rich PS-*b*-PMMA" and the PS matrix in "PS-rich PS-*b*-PMMA." We demonstrated selective doping of CMTE into the PS regions of PS-*b*-PMMA.

1. Introduction

Nanotechnology is based on the ability to create and manipulate materials, devices, and systems on the nanometer scale.[1,2] A "top-down" approach (photo) lithography, which is important for nanopatterning, is widely used to manufacture electronic, optical, and mechanical devices. However, because of its optical limits, etching features with sizes smaller than 100 nm becomes increasingly difficult.[1,3]

In contrast, "bottom-up" processes utilize the interactions between each isolated molecule (or atom), known as the phenomena of "self-organization"[4−6] and "molecular recognition",[7,8] for the fabrication of nanostructural materials. Recently, this approach has attracted a great deal of attention for the fabrication of nanofunctional materials and to add functions to nanostructures measuring less than 100 nm.[1,3]

For example, when one of the side chains of a diblock copolymer, consisting of two different kinds of polymer chains connected by a chemical bond, is replaced with a photochromic molecule, the diblock copolymer molecule will undergo self-organization to form spherical, cylindrical, and lamellar regions[6,9−12] containing various

* To whom correspondence should be addressed. Phone: ++81-72-751-7884. Fax: ++81-72-751-9637. E-mail: chem42@ni.aist.go.jp.
† Photonics Research Institute.
‡ Nanotechnology Research Institute.

(1) Timp, G., Ed. *Nanotechnology*; Springer-Verlag: New York, 1999.
(2) Balzani, V.; Credi, A.; Raymo, F. M.; Stoddart, J. F. *Angew. Chem. Int. Ed.* **2000**, *39*, 3348−3391.
(3) Hey, N. *IEE Rev.* **2003**, *49*, 46−48.
(4) Aizenberg, T.; Black, A. J.; Whitesides, G. M. *Nature* **1999**, *398*, 495−498.
(5) Bain, C. D.; Evall, J.; Whitesides, M. *J. Am. Chem. Soc.* **1989**, *111*, 7155−7164.
(6) Kim, S. O.; Solak, H. H.; Stoykovich, M. P.; Ferrier, N. J.; Pablo, J. J.; Nealey, P. F. *Nature* **2003**, *424*, 411−414.
(7) Gorman, C. *Nature* **2002**, *415*, 487−488.
(8) Shinkai, S.; Ikeda, M.; Sugasaki, A.; Takeuchi, M. *Acc. Chem. Res.* **2001**, *34*, 494−503.
(9) Asakawa, K.; Hiraoka, T. *Jpn. J. Appl. Phys.* **2002**, *41*, 6112−6118.
(10) Hayakawa, T.; Horiuchi, S.; Shimizu, H.; Kawazoe, T.; Ohtsu, M. *J. Polym. Sci. Polym. Chem.* **2002**, *40*, 2406−2414.
(11) Horiuchi, S.; Sarwar, M. I.; Nakao, Y. *Adv. Mater.* **2000**, *12*, 1507−1511.
(12) Horiuchi, S.; Fujita, T.; Hayakawa, T.; Nakao, Y. *Langmuir* **2003**, *19*, 2963−2973.

10.1021/cm049557u CCC: $27.50
Published on Web 08/17/2004

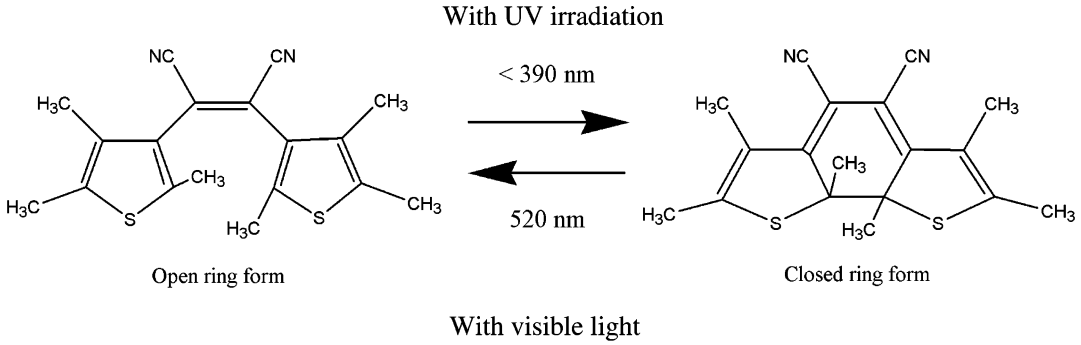

Figure 1. Chemical structure of CMTE: (a) open-ring form; (b) closed-ring form.

functional groups.[12] This is known as the "synthesis process".

As this "synthesis method" requires not only complicated syntheses, but also does not always result in self-organization of the material, very few diblock copolymers with photochromic functional compounds are available. The "doping" process is an alternative approach to introduce photochromic properties into self-organized diblock copolymers.

One doping method consists of dipping the diblock copolymer into solutions[13] of photochromic molecules. Although this is a commonly used method, the residual solvents evaporate very rapidly, which causes damage to the copolymers and induces Rayleigh scattering when irradiated with laser light. In addition to these disadvantages, photochromic molecules tend to be crystallized[14] in solution,[15] and therefore the diblock copolymers do not exhibit their specific photochromic properties. As an alternative, we present the "vapor transportation method"[16] which consists of vaporization of photochromic compounds to prevent isolated single molecules from aggregating into small particles. Although the kinetic energy of a vapor is extremely large, this is an ideal method for selective doping of individual photochromic molecules into specific nanostructures.

In previous studies, we developed the vapor transportation method using the vacuum technique,[16−22] which can form functional molecule-doped polymer regions on polymer substrates.[16−18] We have also succeeded in fabricating opto-electric devices, such as optical transportation media[19] and optical memory media.[20,21] In this paper, we describe how our simple method can change nanostructural materials to nanofunctional materials.

We have already shown that the molecules of the photochromic compound *cis*-1,2-dicyano-1,2-bis(2,4,5-trimethyl-3-thienyl) ethene (CMTE) can be doped more easily into polystyrene (PS) substrates than into poly(methyl methacrylate) (PMMA) substrates. We note that CMTE, one of the derivatives of diarylethene,[23] shows stable and reversible photoisomerization,[14,24] as illustrated schematically in Figure 1. The affinity, called the "$\pi-\pi$ interaction," (reported by Hunter et al.,[25] Jorgensen et al.,[26] and Tsuzuki et al.[27]) between CMTE and polymer substrates may enhance CMTE doping. Optical microscopy, SEM/energy-dispersive X-ray (EDX), FT-IR, and energy-filtering TEM (EF-TEM) analyses[28−32] were performed to demonstrate selective doping of CMTE into nanostructures of PS-*block*-PMMA (PS-*b*-PMMA).

2. Experimental Section

2.1. Materials and Specimen Preparation. CMTE (Tokyo Chemical Industry Co., Ltd.) was used as a photochromic compound without further purification. Pellets of polystyrene (PS) (Aldrich Chemical Co., Inc.; M_w 280 000), poly(methyl methacrylate)(PMMA) (Asahi Kasei Co., Inc.; M_w 140 000−150 000), and polycarbonate (Aldrich; M_w 64 000) were purified by reprecipitation twice from 1,2-dichloroethane solution to methanol, and then molded into a cylindrical shape 2.5 mm in diameter and 3 mm long. Fine powders (with an average diameter of 3 μm) of poly(phenyl methacrylate) (PPhMA) (Scientific Polymer Products, Inc.; M_w 100 000), PMMA (Aldrich ; M_w 15 000), poly(*tert*-butyl methacrylate) (Aldrich; M_w 170 000), poly(4-methylstyrene) (Scientific Polymer Products, Inc.; M_w, 70,000), and poly(p-*tert*-butylstyrene) (Scientific Polymer Products, Inc.; average M_w 50 000−10 0000) were prepared by grinding in a mortar and were heated in ultrahigh vacuum (UHV) chamber at 95 °C for 2 days to remove residual solvent and water.[33]

Two different kinds of diblock copolymers, PS-rich PS-*b*-PMMA and PMMA-rich PS-*b*-PMMA (Polymer Source Inc.), were used without further purification. The number-average

(13) Mori, Y.; Saito, R. *Polymer* **2004**, *45*, 95−100.
(14) Kawai, T.; Koshido, T.; Yoshino, K. *Appl. Phys. Lett.* **1995**, *67*, 795−797.
(15) Biju, V.; Takeuchi, M.; Umemura, K.; Gad, M.; Ishikawa, M. *Jpn. J. Appl. Phys.* **2002**, *41*, 1579−1586.
(16) Hiraga, T.; Chen, G.; Tsujita, K.; Tanaka, N.; Chen, Q.; Moriya, T. *Mol. Cryst. Liq. Cryst.* **2000**, *344*, 211−216.
(17) Mizokuro, T.; Mochizuki, H.; Yamamoto, N.; Tanaka, N.; Horiuchi, S.; Hiraga, T. *J. Photopolym. Sci. Technol.* **2002**, *15*, 137−140.
(18) Mizokuro, T.; Mochizuki, H.; Yamamoto, N.; Tanaka, N.; Horiuchi, S.; Tanigaki, N.; Hiraga, T. *Proc. SPIE* **2003**, *4991*, 333−340.
(19) Mochizuki, H.; Mizokuro, T.; Yamamoto, N.; Tanigaki, N.; Hiraga, T.; Tanaka, N. *Jpn. J. Appl. Phys.* **2003**, *42*, L613−615.
(20) Mizokuro, T.; Mochizuki, H.; Mo, X. L.; Horiuchi, S.; Tanaka, N.; Tanigaki, N.; Hiraga, T. *Jpn. J. Appl. Phys.* **2003**, *42*, L983−985.
(21) Mochizuki, H.; Mizokuro, T.; Tanigaki, N.; Hiraga, T.; Tanaka, N. *Polym. J.* **2003**, *35*, 535−538.
(22) Mizokuro, T.; Mochizuki, H.; Yamamoto, N.; Horiuchi, S.; Tanigaki N.; Hiraga, T. *J. Photopolym. Sci. Technol.* **2003**, *16*, 195−198.
(23) Irie, M., Ed. *Photoreactive Materials for Ultrahigh-Density Optical Memory*; Elsevier: Amsterdam, 1994.
(24) Kawai, T.; Koshido, T.; Kaneuchi, Y.; Yoshino, K. *Thin Solid Films* **1996**, *273*, 195−198.
(25) Hunter, C. A.; Sanders, J. K. M. *J. Am. Chem. Soc.* **1990**, *112*, 5525−5534.
(26) Jorgensen, W. L.; Severance, D. L. *J. Am. Chem. Soc.* **1990**, *112*, 4768−4774.
(27) Tsuzuki, S.; Uchimaru, T.; Matsumura, K.; Mikami, M.; Tanabe, K. *Chem. Phys. Lett.* **2000**, *319*, 547−554.
(28) Reimer, L., Ed. *Energy-Filtering Transmission Electron Microscopy*; Springer-Verlag: Berlin, 1995.
(29) Brown, L. M. *Nature* **1993**, *366*, 721.
(30) Muller, D. A.; Tzou, Y.; Raj, R.; Silcox, J. *Nature* **1993**, *366*, 725−727.
(31) Batson, P. E. *Nature* **1993**, *366*, 727−728.
(32) Horiuchi, S.; Yase, K.; Kitano, T.; Higashida, N.; Ougizawa, T. *Polym. J.* **1997**, *29*, 380−383.

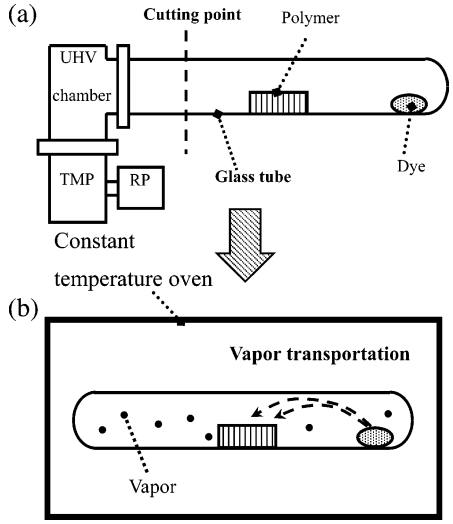

Figure 2. Schematic illustration of the "vapor transportation method" for doping CMTE: (a) vacuum pumping system; (b) heating process after preparing ampules containing polymer substrates with 5 mg of CMTE. During the heating process, the polymer substrates are exposed to CMTE vapor inside the ampules.

molecular weights (M_n) of PS and PMMA in PS-rich PS-*b*-PMMA were 163 500 and 67 200, respectively, with the M_w/M_n ratio of 1.19. The M_n values of PS and PMMA were 29 200 and 285 100, respectively, in PMMA-rich PS-*b*-PMMA, with an M_w/M_n ratio of 1.08. Films of these diblock copolymers were prepared by dissolving 0.2 g of PS-*b*-PMMA in 10 cm^3 of toluene and then pouring the solution into an aluminum Petri dish 5 cm in diameter. The solution was dried under ambient conditions overnight, and then on a hotplate at 50 °C for 1 day, followed by complete dehydration in a vacuum oven at 100 °C for 2 days.[11,12] The thickness of these films was 100 μm.

2.2. Experimental Procedures of the Vapor Transportation Method. The molded substrates and powders were loaded into Pyrex glass tubes with a small amount of CMTE (5 mg), and the pressure in the tube was reduced to the base pressure of 2×10^{-6} Pa, using a vacuum pump as illustrated in Figure 2a. To seal an ampule at the cutting point, a gas burner was used to fuse the cut end. These ampules containing 5 mg of CMTE were heated uniformly at temperatures between 95 and 110 °C as illustrated in Figure 2b and then cooled slowly over several hours.

2.3. Evaluation Procedure. To examine the photoisomerization of CMTE-doped PS, PC, and PMMA molds, a xenon lamp (LAX100, 100 W; Asahi Spectra Co. Ltd.) equipped with mirror modules was used. As illustrated in Figure 1, the chemical structure of CMTE can be altered from the open-ring form to the closed-ring form when irradiated with UV light. In contrast, irradiation with visible light can induce the reverse alteration from the closed-ring form to the open-ring form. A UV-pass mirror module (wavelength between 240 and 300 nm), UVB240-300 nm (Asahi Spectra Co. Ltd.) was attached to the LAX100 when irradiation was performed with UV light. A visible-pass mirror, VIS400-700 nm (Asahi Spectra Co. Ltd.) with a yellow filter (Y-48, Toshiba Glass Co. Ltd.) was attached to the LAX100 when visible light was used for irradiation.

To analyze the depth and interfacial structure of the CMTE-doped regions, samples were prepared by trimming the substrate perpendicular to the surface of the longitudinal molds with razor blades. After UV irradiation for 2 min, samples were observed with an Olympus BH2-RFCA optical microscope. To examine the interface structures of the CMTE-containing region in detail, the surfaces of samples, trimmed using razor blades, were smoothed using an ultramicrotome (Ultracut UCT, Leica) with a glass knife, and then treated by osmium coating using a plasma coating device (PMC-5000; Meiwa-Shoji Co. Ltd.) with an ampule chamber of osmium oxide. Field emission (FE) SEM (Hitachi S-5000) equipped with EDX (Horiba EMAX-5770W) was operated at an acceleration voltage of 20 kV. Mapping images and intensity profiles of sulfur in these samples were obtained.

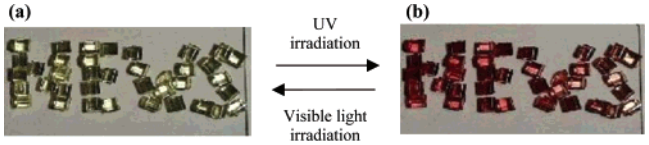

Figure 3. Photographs of CMTE-doped PC molds: (a) after visible light irradiation for 2 min; (b) after UV irradiation for 2 min.

To measure the saturated concentrations of doped-CMTE in polymer powders, FT-IR spectroscopic studies were performed using a Bio-Rad FTS-175C IR spectrometer equipped with an MCT detector. All the spectra were measured at room temperature (23 °C). For the FT-IR measurements, CMTE was doped into the polymer powders of PPhMA, PMMA, poly(*tert*-butyl methacrylate), PS, poly(4-methylstyrene), and poly(p-*tert*-butylstyrene) (~3 μm in diameter) at 95 °C for 168 h. Then, 2 mg of each sample was mixed with 150 mg of potassium bromide (KBr) powder (FT-IR grade; Aldrich) by grinding the two powders in a mortar. The mixtures were compressed into tablet casts with an internal diameter of 10 mm using a tablet machine. After FT-IR measurements, the thicknesses of polymer tablets were measured with a Sony M30 digital micrometer, to evaluate concentrations of CMTE in the tablets.

To obtain zero-loss TEM images, CMTE-doped PS-*b*-PMMA films were cut perpendicular to the surface on an ultramicrotome (RMC MT-XL; Boeckeler Inst., Inc.) with a diamond knife after embedding in light-cured resin (D-800; JEOL DATUM Co. Ltd.). Ultrathin sections of 50 nm were collected on a 600 mesh copper grid. Then, a LEO 922 OMEGA energy filtering TEM (EF-TEM) was used to examine the specimens at an acceleration voltage of 120 kV.

3. Results and Discussion

3.1. Photoisomerization of CMTE-Doped Polymer Molds. As shown in Figure 3a and b, the color of CMTE-doped PC molds changed from light yellow to reddish brown when irradiated with UV light for 2 min. This change confirmed that the chemical structures of CMTE doped in PC molds were transformed from the open- to the closed-ring form by UV irradiation. In contrast, the color of these molds changed from reddish brown to light yellow when irradiated with visible light for 2 min. This phenomenon is known as "photoisomerization of CMTE",[14, 24] as illustrated in Figure 1. We observed the same change of color on UV irradiation of CMTE-doped PS and PMMA molds (data not shown). Repeated photoisomerization of CMTE-doped PS, PC, and PMMA molds was confirmed at least 25 times by the color change of CMTE at 25 °C in a 1 atm air atmosphere. These results implied that CMTE molecules retain their own photochromic properties inside the polymer molds; our new method simply adds the photochromic properties of CMTE molecules to their surfaces.

3.2. Observation of CMTE-Doped Regions in Polymer Molds. To evaluate CMTE doping rates, we first used optical microscopy to observe the interfacial structures between CMTE-doped regions and the PS, PC, and PMMA substrates. Figure 4a, b, and c show low magnification images of CMTE-doped PS, PC, and PMMA molds exposed to CMTE vapor at 110 °C for 26 h, 105 °C for 24 h, and 105 °C for 24 h, respectively.

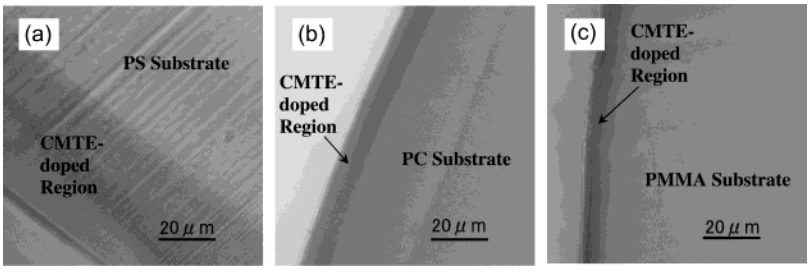

Figure 4. Low-magnification images of CMTE-doped polymer molds observed by optical microscopy: (a) PS molds exposed to CMTE vapor at 110 °C for 26 h; (b) PC molds exposed to CMTE vapor at 105 °C for 24 h; and (c) PMMA molds exposed to CMTE vapor at 105 °C for 24 h.

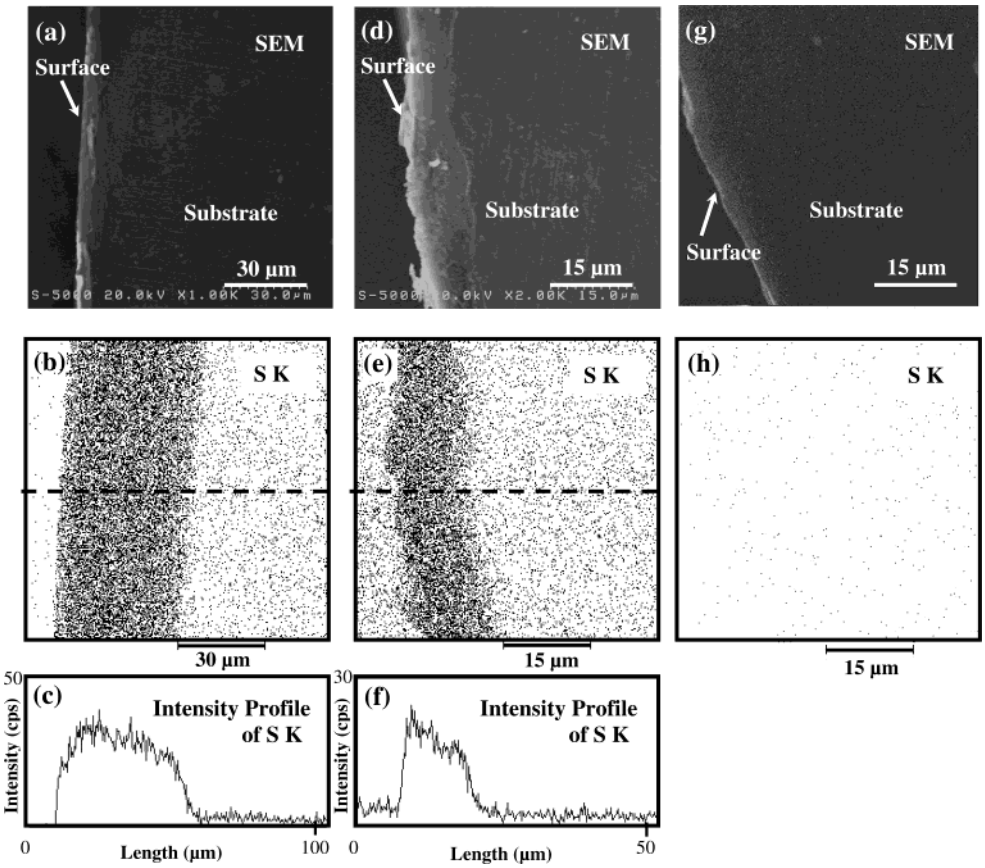

Figure 5. SEM images, S Kα images, and intensity profiles of cross-sections of CMTE-doped PS molds by SEM equipped with EDX elemental analysis. SEM/EDX was operated at an acceleration voltage of 20 kV for a scan time of 1200 s. (a), (b), and (c) show PS molds exposed to CMTE vapor at 110 °C for 26 h (the same as Figure 4a). (d), (e), and (f) show samples treated at 95 °C for 24 h. (g) and (h) show PS substrate containing no CMTE. (a), (d), and (g) are SEM images. (b), (e), and (h) are S Kα images. (c) and (f) show intensity profiles of S Kα. Dashed lines in both (b) and (e) show the locations from which the intensity profiles of S Kα in (c) and (f) were taken, respectively. The full ranges of the Y-axes in (c) and (f) are 50 and 30 cps, respectively. The dark areas on the S Kα images in (b) and (e) indicate the presence of CMTE molecules in PS molds.

The interfacial regions of the doped CMTE were determined from their color. Figure 4 shows reddish brown regions, the interfaces of which have rapid CMTE concentration decreases. Assuming that their interfaces have the rapid concentration decreases, the depths of CMTE doped in PS, PC, and PMMA were estimated to be 43.7, 10.0, and 7.5 μm, respectively.

Next, we investigated the interfacial structures in CMTE-doped PS molds with FESEM/EDX. Figure 5a, b, and c show PS substrate exposed to CMTE vapor at 110 °C for 26 h (same as Figure 4a). Figure 5d, e, and f show CMTE-doped PS treated at 95 °C for 24 h. Next, Figure 5g and h show PS substrate containing no CMTE. Figure 5a, d, and g are SEM images, and Figure 5b, e, and h are images of S Kα. Figure 5c and f present the intensity profiles of S Kα. As a single CMTE molecule contains two sulfur (S) atoms (see Figure 1) and these polymer molds do not contain S atoms, we expected to detect S Kα element signals in doped CMTE of the sample in Figure 5a and d with SEM/EDX elemental analysis. The SEM images in Figure 5a, d, and g do not show the presence of CMTE-doped interfacial regions. However, the dark areas in S Kα images in Figure 5b and e demonstrate the presence of CMTE molecules in the PS substrate, and Figure 5h demonstrates the lack of CMTE. In Figure 5c, we measured the width of the doped CMTE in PS as 47.8 μm. Figure 5c shows that the intensity of S Kα decreased gradually from the surface to a depth of 41.4 μm, and then dropped abruptly at an interfacial distance of 6.4 μm. The

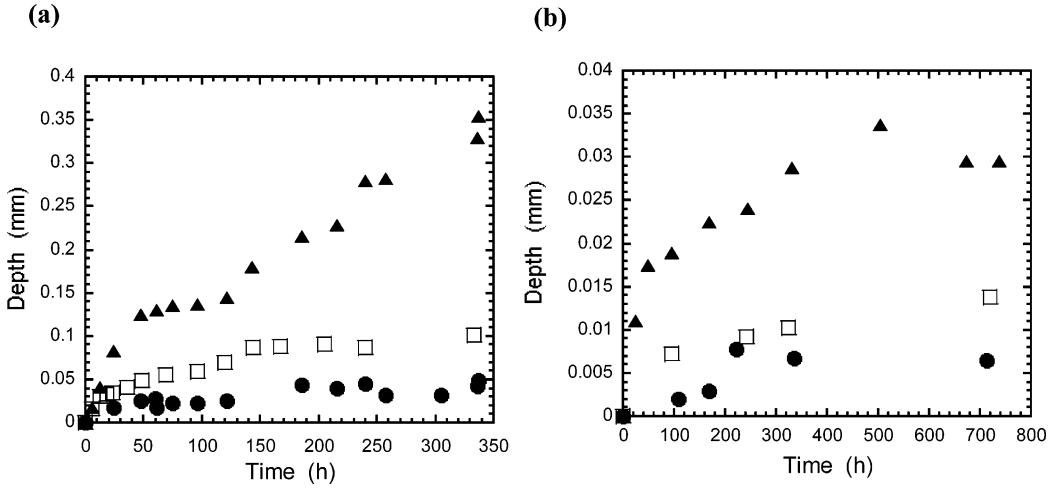

Figure 6. Growth depths of CMTE-doped regions in PS (closed triangles), PMMA (closed circles), and PC (open squares) substrates as a function of doping time at 110 °C (plot (a)) and 95 °C (plot (b)).

intensity profile of S Kα in Figure 5c and f agreed with the depth of the region shown the S Kα images in Figure 5b and e and with the results of optical microscopy, which suggested that the depth of the CMTE-doped region can be distinguished by simple optical observation. Figure 5c shows that the interface with the PS substrate has a rapid concentration decrease. Figure 5f shows that the thickness of the doped region of CMTE was 15.0 μm, which was smaller than that in Figure 5c. The intensity of S Kα decreased gradually from the surface to a depth of 11.8 μm and then dropped abruptly at a further distance of 3.2 μm, implying that the interface also has a rapid concentration decrease structure. Similarly, we observed the same rapid concentration decrease structure of CMTE-doped PC and PMMA interface regions (data not shown). When CMTE was doped to deeper levels, a CMTE-doped region with a rapid concentration decrease extended deeper from the surface.

If doping of CMTE molecules follows Fick's laws of diffusion, then we should see a profile of S Kα with a gradual concentration gradient[34] instead of a rapid concentration decrease. At present, our results suggest that Fick's laws of diffusion do not govern doping of CMTE into polymer substrates: that is, doping behavior is not mediated by conventional thermal diffusion as described in ref 34.

3.3. CMTE-Doping Rates into PS, PC, and PMMA Molds. In section 3.2, we estimated the thickness of the CMTE-doped regions observed by optical microscopy. In this section, we estimated CMTE doping rates into PS, PC, and PMMA by measurement of the depth as a function of doping time and temperature.

Figure 6 a and b show the growth depths of CMTE-doped regions in PS (closed triangles), PMMA (closed circles), and PC (open squares) substrates as a function of doping time at 110 and 95 °C, respectively. In PC 20 min was required to form ~1 μm of a CMTE-doped region at 110 °C and around 0.5 μm at 95 °C. By 240 h, the depth of doped regions in PS reached 0.28 mm at 110 °C and 0.024 mm at 95 °C. By 96 h at 110 °C, the depths of doped regions in PS, PC, and PMMA were 0.14, 0.059, and 0.022 mm, respectively. The differences in formation rate between PS, PC, and PMMA were independent of doping temperature although the formation rate of CMTE-doped regions of each polymer seemed to be largely dependent on doping temperature.[22] The doping rate of PC was greater than that of PMMA although glass transition temperatures (T_g) of PC and PMMA were 150 and 105 °C, respectively, implying that the effect of T_g may not play an important role in the differences in formation rate between PS, PC, and PMMA.

The intermolecular interaction between aromatic rings, called the $\pi-\pi$ interaction, influences the three-dimensional structures of proteins and DNA as well as the crystal packing of molecules containing aromatic rings.[25−27] As CMTE molecules possess π-electrons, and side chains of PS and principal chains of PC possess aromatic groups, the $\pi-\pi$ interactions can enhance the affinity between CMTE and these polymers. The $\pi-\pi$ interaction between phenyl groups of the organic polymer and those of silica gel may play an important role in the synthesis of homogeneous polymer hybrids of aromatic polymers, polystyrenes, and silica gel.[35] In particular, water-absorptivity of PS is lower than those of PC and PMMA.[36] Due to the high degree of hydrophobicity of PS, the $\pi-\pi$ interactions between CMTE and side chains of PS are stronger than those between CMTE and the principal chains of PC. We concluded that the differences in doping rates might have been due to the differences in their hydrophobic properties and the $\pi-\pi$ interactions of CMTE.

3.4. Saturated Concentrations of CMTE in PS, PMMA, and Their Derivatives. Quantitative studies of saturated concentrations of CMTE were performed by FT-IR to characterize the interactions between CMTE and PS, PMMA, the two PS derivatives poly(4-methylstyrene) and poly(*p*-*tert*-butylstyrene), and the two PMMA derivatives poly(phenyl methacrylate) (PPh-

(33) Hiraga, T.; Yamasaki, Y.; Tanaka, N.; Hayamizu, K.; Moriya, T. *Chem. Lett.* **1993**, 1791−1794.
(34) Atkins, P. W., Ed. *Physical Chemistry*, 5th ed.; Oxford University Press: Oxford, 1998.
(35) Tamaki, R.; Samura, K.; Chujo, Y. *Chem. Commun.* **1998**, 1131−1132.
(36) The Japan Society for Technology of Plasticity, Ed. *Plastic Processing Databook*, 2nd ed.; The Nikkan Kogyo Shimbun: Tokyo, 2002; p 16.

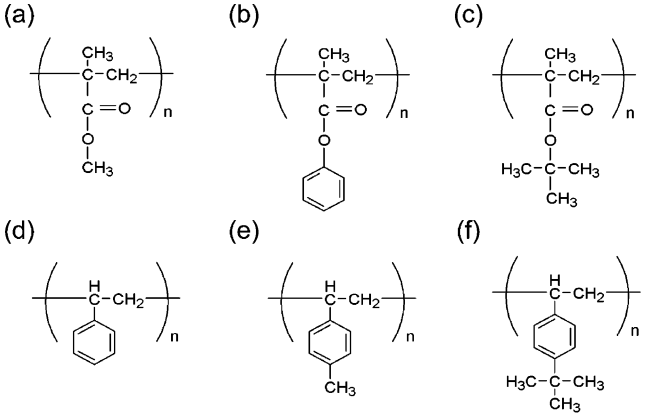

Figure 7. Chemical structures of PMMA and PS derivatives: (a) PMMA; (b) poly(phenyl methacrylate); (c) poly(*tert*-butyl methacrylate); (d) PS; (e) poly(4-methylstyrene); and (f) poly(*p*-*tert*-butylstyrene).

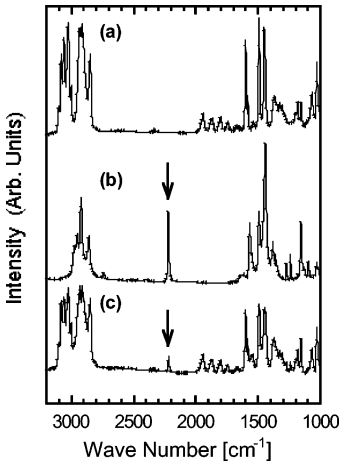

Figure 8. FT-IR spectra of PS substrate (thickness, 20 μm) (spectrum (a)), CMTE powder mixed (0.705 wt %) with a KBr tablet (spectrum (b)), and a CMTE-doped PS powder mixed with a KBr tablet (spectrum (c)). The wavenumber resolution was 2 cm^{-1}. No signal was observed at around 2220 cm^{-1} in spectrum (a). However, peaks were detected at around 2220 cm^{-1} in both spectra (b) and (c) (see arrows).

MA) and poly(*tert*-butyl methacrylate). Figure 7 shows the chemical structures of these polymers.

Figure 8 shows FT-IR spectra of a PS substrate (thickness, 20 μm) (spectrum (a)), CMTE powder mixed (0.705 wt %) with a KBr tablet (spectrum (b)), and CMTE-containing PS powder mixed with a KBr tablet (spectrum (c)). No signals were observed at around 2220 cm^{-1} in spectrum (a). However, peaks were detected at around 2220 cm^{-1} in both spectra (b) and (c) (see arrows in Figure 8), which imply C≡N stretching modes derived from CMTE molecules. We evaluated CMTE concentrations in powders of PS, PMMA, and their derivatives, assuming that CMTE was doped uniformly into these polymer powders. As shown in Table 1, glass transition temperatures (T_g) of 6 different kinds of polymer powders before CMTE doping were measured by differential scanning calorimetry (DSC), and CMTE concentrations after doping at 95 °C for 168 h were measured by FT-IR. We note here that the CMTE concentrations, which were evaluated from weight loss of polymers by thermogravimetry (TG) in a vacuum,[37] agreed with those of CMTE determined by FT-IR.

Table 1. CMTE Concentrations Estimated by FT-IR of 6 Different Kinds of Polymer Powders after Doping at 95 °C for 168 H, and Glass Transition Temperatures (T_g) Measured by Differential Scanning Calorimetry (DSC) of the Powders before Doping

polymer	concn (wt %)	T_g[a] (°C)
PMMA	6.7	105
poly(phenyl methacrylate)	11.0	110
poly(*tert*-butyl methacrylate)	2.7	107
PS	11.6	100
poly(4-methylstyrene)	2.6	106
poly(*p*-*tert*-butylstyrene)	1.4	132

[a] T_g: Glass transition temperature of polymer before CMTE doping.

Results obtained by DSC indicated the homogeneous dispersion of CMTE doped into polymer powders, which implied that the concentration of CMTE measured by FT-IR is equivalent to its saturated concentration.

The concentration of CMTE in polymers can indicate the diffusivity of CMTE doping. In Table 1, PPhMA and PS, which have phenyl groups in their side chains (as shown in Figure 7b and d, respectively), show the highest CMTE concentrations among the derivatives examined. In contrast, PMMA and poly(4-methylstyrene), which have methyl groups at the ends of their side chains (Figure 7a and e), have lower CMTE concentrations than those of PPhMA and PS, respectively. Poly (*tert*-butyl methacrylate) and poly(*p*-*tert*-butylstyrene), which have *tert*-butyl groups at the ends of their side chains (Figure 7c and f), have the lowest CMTE concentrations among the derivatives examined. Although PPhMA has a high packing density among PMMA derivatives (PPhMA > PMMA > poly(*tert*-butyl methacrylate)),[38] the CMTE saturated concentration in PPhMA was the highest, implying that PPhMA has the highest diffusivity among those examined. These results indicated that the affinity between CMTE molecules and phenyl groups in their side chains, as mentioned in Section 3.3, increases saturated concentration of CMTE in PPhMA and PS.

3.5. Selective Doping of CMTE into Nanophase-Separated Structures of PS-*b*-PMMA Films. In this section, we discuss the selectivity of doped CMTE in PS nanophase-separated structures of PS-*b*-PMMA.

Figure 9a and b show ultrathin section EF-TEM images of a CMTE-doped PS-rich PS-*b*-PMMA film and a CMTE-doped PMMA-rich PS-*b*-PMMA film (see Section 2), respectively, after treatment at 130 °C for 12 h. In Figure 9a, PMMA domains were isolated in the PS matrix. In Figure 9b, PS domains were isolated in the PMMA matrix. In Figure 9a, the dark regions due to elastic scattering of electrons by sulfur (S) atoms in CMTE molecules represent the distribution of CMTE doped into the PS matrix. The white dots with a diameter of 20 nm indicate the isolated PMMA domains. In Figure 9b, the black dots ~20 nm in diameter represent the distribution of CMTE doped into PS domains, surrounded by PMMA matrix.

The lower "affinity" of PMMA against CMTE, as mentioned in Sections 3.3 and 3.4, causes CMTE to

(37) Mizokuro, T.; Mochizuki, H.; Mo, X. L.; Tanigaki, N.; Hiraga, T. Submitted to *Mol. Cryst. Liq. Cryst.*

(38) Brandrup, J., Immergut, E. H., Grulke, E. A., Ed. *Polymer Handbook*, 4th ed.; John Wiley & Sons Inc.: New York, 1999.

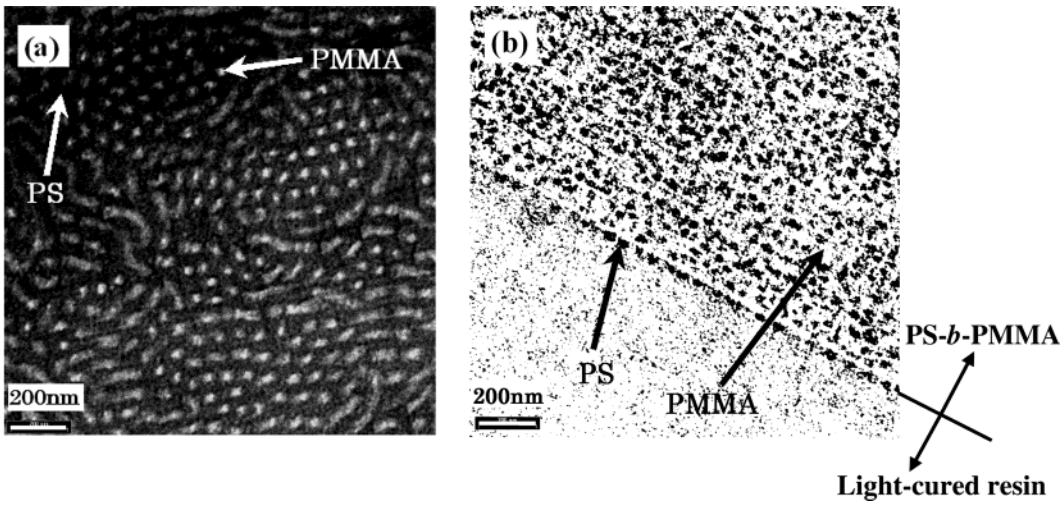

Figure 9. Ultrathin section EF-TEM images of a CMTE-doped "PS-rich PS-*b*-PMMA" film (a) and a CMTE-doped "PMMA-rich PS-*b*-PMMA" film (b) after treatment at 130 °C for 12 h. The dark regions due to elastic scattering of electrons by sulfur (S) atoms in CMTE molecules indicate the distribution of CMTE doped in PS regions. The white regions represent the PMMA regions.

avoid PMMA, while being attracted to PS. Our observations demonstrated the precise control of localization of CMTE doping into PS nanophase-separated structures of PS-*b*-PMMA films.

4. Conclusions

CMTE-doped molds and powders of PPhMA, PMMA, poly(*tert*-butyl methacrylate), PS, poly(4-methylstyrene), poly(*p*-*tert*-butylstyrene), and PC were formed by the vapor transportation method. The photochromic properties and interfacial structures of CMTE-doped polymers were examined by a combination of optical microscopy and SEM/EDX analysis. Rapid CMTE concentration decreases were observed at the interfaces of these polymers, confirming the photoisomerization of CMTE. As the results of SEM/EDX analysis agreed with those of optical microscopy, this combination of analyses is a simple but elegant method for screening of CMTE-doped polymer substrates.

The thicknesses of CMTE-doped regions of PS, PC, and PMMA could be determined by adjusting the doping time and temperature. CMTE-doping rates, and CMTE saturated concentrations were dependent on the strength of the $\pi-\pi$ interaction between CMTE and polymer substrates. We have observed CMTE-doped nanodomains of PS-*b*-PMMA with absorption spectra by scanning near-field optical microscopy (SNOM).[39] If the absorption coefficient and the transmissivity of CMTE-doped nanodomains can be altered by irradiation with UV or visible light with SNOM,[40−44] the CMTE-doped nanodomains of PS-*b*-PMMA might be useful for fabrication of ultrahigh-density rewritable optical recording media. As reported here, we found that CMTE can be doped selectively into PS-nanophase-separated structures in PS-*b*-PMMA, which is known as a binary system polymer. However, we have yet to investigate the mechanism of diffusion that controls the intensity gradients. As diarylethenes, such as CMTE, have the advantages of thermal irreversibility, fatigue-resistance, and high sensitivity,[23] our vapor transportation method can provide a unique surface modification process for polymer substrates used to fabricate optical devices, such as memory media for optical recording and optical switching.[45]

In future studies, we will investigate methods to control the thickness and interface structures of doped organic compounds with low molecular weights by adjusting the optimal combination between polymer substrates and organic compounds. These will include organofluorine compounds, other photochromic dyes, fluorescent dyes, and charge-transporters, to provide a new fabrication process for organic optoelectronic devices, such as optical transportation media, memory media, and light-emitting devices.

Acknowledgment. We thank Dr. Keiko Tawa of the Research Institute for Cell Engineering of AIST for help with the FT-IR analysis. We also thank Dr. Takahisa Taguchi, the deputy director of the Research Institute for Cell Engineering of AIST, for the provision of laboratory facilities. Furthermore, we also thank Dr. Norio Tanaka of Dainichiseika Color and Chemicals Manufacturing Co., Ltd., for discussing deeply about this work. This work was supported in part by a grant for the support of young researchers from the Ministry of Education, Culture, Sports, Science, and Technology (MEXT) of Japan.

CM049557U

(39) Yamamoto, N.; Mizokuro, T.; Mochizuki, H.; Horiuchi, S.; Hiraga, T. *J. Microsc.* **2004**, *213*, 135−139.
(40) Ash, E. A.; Nicholls, G. *Nature* **1972**, *237*, 510.
(41) Pohl, D. W.; Dank, W.; Lanz, M. *Appl. Phys. Lett.* **1984**, *44*, 651−653.
(42) Betzig, E.; Chichester, R. J. *Science* **1993**, *262*, 1422−1425.
(43) Irie, M.; Ishida, H.; Tsujioka, T. *Jpn. J. Appl. Phys.* **1999**, *38*, 6114−6117.
(44) Kim, M. S.; Sakata, T.; Kawai, T.; Irie, M. *Jpn. J. Appl. Phys.* **2003**, *42*, 3676−3681.
(45) Irie, M.; Fukaminato, T.; Sasaki, T.; Tamai, N.; Kawai, T. *Nature* **2002**, *420*, 759−760.